Universality of evolutionary dynamics with arbitrary demography

Andrea Mazzolini[1,2] and Jacopo Grilli[2,*]

[1] *Laboratoire de physique de l'École normale supérieure (PSL University), CNRS, Sorbonne Université, and Université de Paris, 75005 Paris, France*

[2] *The Abdus Salam International Centre for Theoretical Physics (ICTP), Strada Costiera 11, 34014 Trieste, Italy*

The assumption of constant population size is central in population genetics. It led to a large body of results, which have proven successful to understand evolutionary dynamics. Part of this success is due to their robustness to modeling choices. On the other hand, allele frequencies and population size are both determined by the interaction between a population and the environment. Including explicitly the demographic factors and life-history traits that determine the eco-evolutionary dynamics makes the analysis difficult and the results dependent on model details. Here, we develop a framework that encompasses a great variety of systems with arbitrary population dynamics and competition between species. By using techniques based on scale separation for stochastic processes, we are able to compute evolutionary properties, such as the invasion probability. Remarkably, these properties assume a universal form with respect to our framework, which depends on only three life-history traits related to the exponential fitness, the invasion fitness, and the carrying capacity of the alleles. In other words, different systems, such as Lotka-Volterra or a chemostat model, share the same evolutionary outcomes after the correct remapping of the parameters of the models into three effective life-history traits. An important and surprising consequence of our results is that the direction of selection can be inverted, with a population evolving to reach lower values of fitness. This can happen because the obtained frequency-dependent noise (affected by the three life-history traits) can generate an effective force that counterbalance classical selection.

Competition is a fundamental agent of natural selection. The scarcity of a resource (a nutrient, water, space, ...) limits the population growth, determining a selection pressure. Variants able to grow faster or more efficiently spread within the population. To quantify these kind of phenomena, the vast majority of results in population genetics are based on the assumption of constant population size [1–8]. The success of this assumption lies in the generality of the results. When the population size is large enough, Kimura's diffusion limit [1, 9] is the convergence point of several alternative models. In fact, while different population genetics models (Wrigh-Fisher [10, 11] , Moran [12], conditional branching processes [13], and some Canning processes [14]) start from radically different assumptions about the genealogical and demographic structure of the population, they share the same predictions, up to a simple rescaling of timescales and parameters. For most of the theoretical advances in population genetics, the total population size is an effective parameter of the model, which should be fitted from data, and the allele frequencies are the only dynamical degrees of freedom.

However, mechanistically, not only the allele frequencies, but also the total population size is determined by the interaction between a population and the environment. Moreover, experimental works [15, 16] suggest that the variation of the population size can play a role in the evolutionary process, implying that its dynamics should not be neglected in theoretical descriptions.

Non-stationary conditions are an important example where the dynamics of population size cannot be neglected to

*Electronic address: jgrilli@ictp.it

understand how evolution — here intended as the dynamics of relative frequencies of alleles — unfolds. For instance range expansions leave strong signature on the genetic diversity of a population [17–19]. Here we instead focus on the equally non-trivial scenarios where the total population is stationary, but not constant and not independent of allele frequencies, over the timescales of population dynamics.

A classical approach to study this problem is to consider the total population size as decoupled from the allele frequency. In this context the dynamics of the total population is assumed a-priori [20–23]. The alternative is to model explicitly population dynamics, which requires to choose how environmental constraints limit population growth, leading to different modeling framework, as for instance: Lotka-Volterra [24–30], a generalization of the Moran model [31], or public good models [32, 33].

The increased realism of these models undermines, at least in principle, the generality of the standard population genetics results. To what extent the details of demography and life-history determine the evolutionary outcome?

In this work we address this question by considering a general ecological framework to describe population dynamics. This approach encompasses several alternative models, from Lotka-Volterra to competition in a chemostat, under the same mathematical framework. We show that evolutionary predictions are instead robust and insensitive to the details of population dynamics. Within our framework, evolutionary observables, such as the invasion probability, are universal and depend on only three parameters, related with the concepts of exponential fitness, invasion fitness, and carrying capacity. We first present the general framework, then we show its approximation with the scale separation, and the computation of evolutionary observables. Finally, we conclude with an explicit example of the chemostat model for resource competition, showing how the previous general results can lead to an evolutionary trajectory with decreasing fitness over time.

Results

A model for evolution with a general demographic dynamics

We consider the stochastic dynamics of an heterogeneous population. The birth and death rate of each allele (see Materials and Methods) are determined by allele specific parameters as well as the interaction, through competition, with others. The abundance of each allele n_i as well as the total population size $n = \sum_i n_i$ are therefore changing stochastically over time in a interdependent manner. The deterministic part of the dynamics, obtained by neglecting the diffusion term (see Materials and Methods and Supplementary Materials, section 1), reads

$$\frac{1}{n_i}\frac{dn_i}{dt} = \rho_i \beta\left(\mathbf{n}\right)\left(1 - \frac{\omega\left(\mathbf{n}\right)}{\phi_i}\right) \ , \tag{1}$$

This class of models provides a general description of competing alleles. We restrict our analysis to competition for a single resource, in which case the two functions $\beta(z)$ and $\omega(z)$ are a function of linear combination of abundances only: $z = \sum_i \chi_i n_i / M$.

This framework is in fact quite flexible and it allows to recover commonly used models with specific choices of $\beta(z)$ and $\omega(z)$. The rates in eq. 6 reduces to the classical Moran-model [8] when $\beta(z) = \chi_i = \rho_i = 1$ (the equivalence can be seen from equation (2)). The Lotka-Volterra dynamics is obtained using $\beta(z) = 1$ and $\omega(z) = z$, the chemostat model [34] with $\beta(z) = 1/z$ and $\omega(z) = z$, and the generalized Moran model [31] with $\beta(z) = 1$, $\omega(z) \propto (1 + z)$, and $\chi_i = 1$ (see Materials and Methods for more details and other examples).

The allele dynamics depends on three allele-specific parameters (see Materials and Methods), ρ_i, ϕ_i, and χ_i, and one additional parameter M which sets the scale of the total population size. In absence of population limitation (when $\omega(\mathbf{n})/\phi_i \ll 1$ for all i), the allele i will grow exponentially with growth rate equal to the *exponential fitness* ρ_i. The *competitive strength* χ_i contribute to the carrying capacity in clonal population of allele i, which is equal to $K_i = M\omega^{-1}(\phi_i)/\chi_i$. The invasion fitness ϕ_i determines the growth rate of an invader in presence of an established population: a small population of an invader i in a large population j at carrying capacity has a growth rate proportional to $1-\phi_j/\phi_i$. The growth rate of the mutant is positive if and only if $\phi_i > \phi_j$, implying that the allele with a competitive advantage is the one with the largest *invasion fitness* ϕ.

Therefore, this deterministic analysis shows that, despite the model generality, the evolutionary success of a allele in the long-term is determined only by one parameter: the invasion fitness. In this respect, it is interesting to notice that the exponential fitness, the structure of the interactions as well as how the global population size evolves do not play a role.

This result holds as long as one can consider the population scale M infinite and the "strong" selection regime. Indeed, when the differences between the invasion-fitness parameters are small, such that their product with M is of order one, $M|\phi_i - \phi_j|A/\sum_{k=1}^{A}\phi_k = O(1)$, fluctuations become important and a stochastic description is necessary. This is the "weak" selection regime analysed in the next section.

The effective dynamics in the weak-selection regime is controlled by few parameters

When population sizes are large and fitness differences are small the trajectories can be separated in a fast transient followed by a slow dynamics, as shown in Figure 1. The initial trajectory drives the system to a slow manifold of solutions, which correspond to stationary values of the total population size. What follows is a dynamics constrained on the slow manifold.

The "slow" dynamics is determined by the combination of two forces. The genetic drift is pushing the system away of the manifold of solutions. The deterministic part of the dynamics is pushing the system back to the slow manifold. Since these two forces do not act orthogonally to the manifold, they result in a non-trivial combination, which effectively drive the evolution of the system.

After a non-trivial calculation [35] (see Materials and Methods and Supplementary Materials section 2) one obtain an effective equation, which parallels Kimura's diffusion limit. In the case of two alleles, this effective equation describes the dynamics of the rescaled abundance $y = n_1/K_1$ of one allele, characterized by some values of exponential fitness ρ_1, invasion fitness ϕ_1, and competitive strength χ_1 in the presence of another allele with different traits (ρ_2, χ_2, ϕ_2). The equation reads:

$$\begin{aligned}\frac{dy}{dt} = \frac{y(1-y)}{\bar{r}}\left(s - \frac{1}{K_2\bar{r}}\left(rc - 1 + \frac{r(c-1)}{\bar{r}}\right)\right) + \\ + \sqrt{\frac{y(1-y)}{K_2\bar{r}^2}(rx + c(1-x))}\cdot\eta(t).\end{aligned} \tag{2}$$

where $\eta(t)$ is a white noise term (see Supplementary Materials) and the average $\bar{g}$ is an average over the population (i.e., $\bar{g} = gy + 1 - y$). The dynamics of the rescaled abundance y depends on three parameters in addition to the carrying capacity of the second allele K_2 (of order M): s, r, c. These three parameters are related to the ratios

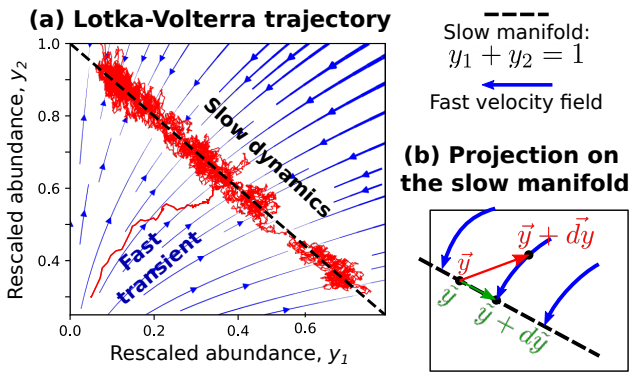

FIG. 1: The panel (a) shows an illustrative example of the time-scale separation in a Lotka-Volterra for two species: $\beta(z) = 1$, $\omega(z) = z$, $M = 2000$, $s_2 = 0.002$. The variables $y_i = n_i/K_i$ are the abundances re-scaled by the carrying capacity. The panel (b) sketches the idea underlying the projection of the dynamics onto the slow manifold: infinitesimal steps outside the manifold (in red) are mapped again on it by the fast velocity field. As a result, to correctly take into account these effects, the increment of the effective variable $\tilde{y}$ (in green) corresponds to the projection of $\vec{dy}$ along the velocity field.

between the life-history trait parameters of the two alleles. In particular, s is the selection coefficient $s = (\phi_1 - \phi_2)/\phi_1$, $r = \rho_1/\rho_2$, and $c = \chi_1/\chi_2$, which, in the weak selection regime, can also be expressed as the ratio of the carrying capacities $c = K_2/K_1$ (see Materials and Methods). From this equation, one can obtain an explicit expression for the dynamics of the relative abundance $x = n_1/(n_1 + n_2) = y/(y + (1 - y)c)$ (see Supplementary Materials).

Equation 2 is the main technical achievement of this paper, from which stem several results. First, it does not depend on the functions $\beta(\cdot)$ and $\omega(\cdot)$, which only determine the timescale of the dynamics (see Supplementary Materials). This implies that systems characterized by very different demographic dynamics will have the same evolutionary trajectories. As a consequence, if the alleles do not differ in their exponential fitness and in the carrying capacities (i.e. if $r = c = 1$) equation 2 reduces to Kimura's diffusion limit. In contrast, when also these life-history traits differ, the the deterministic term depends on the balance between two forces. The first term is proportional to the selection coefficient s. The second one, absent in the classic Kimura's diffusion limit, is proportional to $1/M$ and depends also on allele frequencies. The existence of this second term can lead to radically different evolutionary trajectories. To better quantify this statement, in the next section we calculate the invasion probability.

Carrying capacity, exponential and invasion fitness control the evolutionary success

The evolutionary success of an allele in an environment described by (2) can be quantified by the probability that one individual of a given type is able to invade a population of a second type, i.e the invasion probability. The ratio between the probability of invasion of the first allele $p_{1\ \mathrm{inv}}$ and the invasion of the second one $p_{2\ \mathrm{inv}}$ can be expressed analytically (see Supplementary Materials section 3)

$$\log \frac{p_{1\ \mathrm{inv}}}{p_{2\ \mathrm{inv}}} = sK_2 \frac{r-1}{r-c} + \frac{sK_2 r(c-1) - (1-rc)(r-c)}{(r-c)^2} \log \frac{c}{r} \ , \tag{3}$$

which, in the singular case of $r = c$ becomes $\log(p_{1\ \mathrm{inv}}/p_{2\ \mathrm{inv}}) = \frac{r+1}{r}\left(\frac{sK_2}{2} + 1 - r\right)$.

Despite the generality of the modeling framework (6), this quantity depends on only three parameters: the

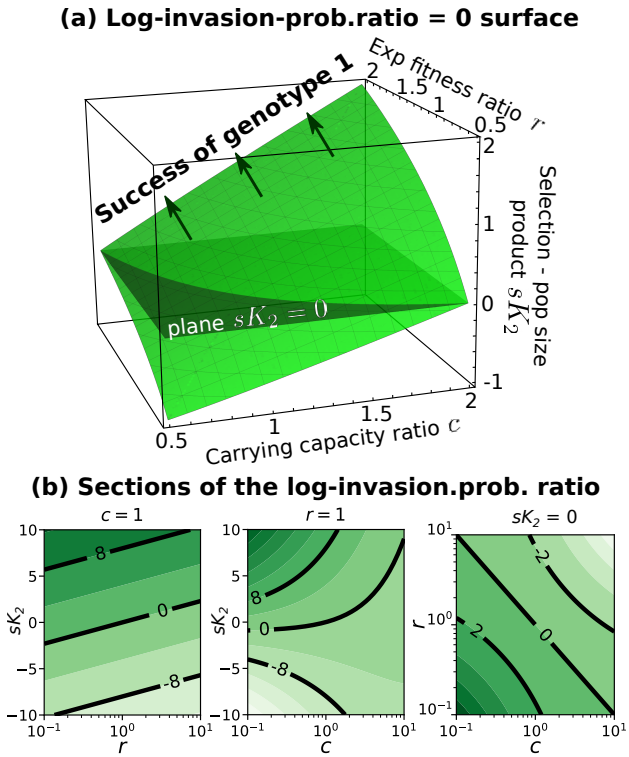

FIG. 2: How the invasion probability depends on the three parameters. Panel (a) shows the surface $\log(p_{1\ \mathrm{inv}}/p_{2\ \mathrm{inv}}) = 0$, panel (b) different sections of the invasion probability log-ratio. A darker shade of green represents a larger ratio.

exponential-fitness ratio r, the (inverse) ratio between the carrying capacities c, and the product between the selection coefficient and the size of the second population at carrying capacity sK_2.

Figure 2a shows the surface at $\log(p_{1\ \mathrm{inv}}/p_{2\ \mathrm{inv}}) = 0$, which separates the regions of parameters between a more successful first allele, $p_{1\ \mathrm{inv}} > p_{2\ \mathrm{inv}}$, and the opposite scenario. Note that, differently from the strong selection regime, here, a "fitter" genotype can have lower invasion fitness, i.e. within the volume below the $s = 0$ plane and above the $\log(p_{1\ \mathrm{inv}}/p_{2\ \mathrm{inv}}) = 0$, surface of the Figure.

In absence of differences in the exponential fitness and carrying capacity (i.e., if $r = c = 1$), one recovers the Kimura's diffusion limit $\log(p_{1\ \mathrm{inv}}/p_{2\ \mathrm{inv}}) = K_2 s$ traditionally obtained under a constant total population size K_2 [8]. Moreover, for $c = 1$ and $s = 0$ one recovers the invasion probability of [31] and [29]. Figure 3 shows numerical simulations of the invasion probability in alternative models, differing for their birth and death rate dependency on the alleles population sizes. The figure shows that once these different models are mapped onto our framework (6), all the invasion probabilities collapse to the same curves as predicted by equation (3). Details about how the simulations are performed are shown in Supplementary Materials, section 3. The definitions of the simulated models and how to map them in our framework, is in Materials and Methods.

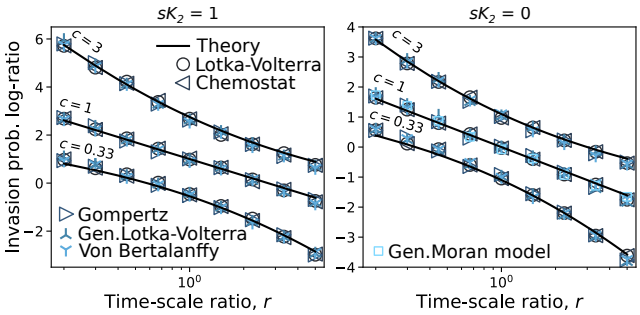

FIG. 3: Collapse of different demographic models on the same invasion probability, given by equation (3), black lines. The simulations consider the competitive Lotka-Volterra, a chemostat model [36], the Gompertz growth dynamics [37, 38], a generalized Lotka-Volterra [39] with exponent $\nu = 1/2$, the Von Bertalanffy model [40] with $\alpha = 2/3$ and the Generalized Moran model [31] which is defined only for $sK_2 = 0$ and $c = 1$. For more details about the models see Materials and Methods.

Invasion probability through mutation

The expected number of mutations per generation depends on the population size. Since in our case the total population size can vary across population compositions, also the total mutation rate depends on which alleles are present and in which abundance. This dependency induces an additional effect of the varying total population on the most likely evolutionary trajectory.

We consider small, allele independent and symmetric mutation probability $\mu \ll 1$. Given, for example, the population 2 at carrying capacity, K_2, the birth and death rates of (6) are balanced (the system is in the steady state), $b_2 = \rho_2 \beta(\omega^{-1}(\phi))K_2$. This quantity defines the generation rate. If one multiplies this rate by the per-capita mutation probability, it obtains the the rate at which a mutant of type 1 appears: μb_2. Therefore, one can compute the probability that the new invader overcomes the resident population in the case it appears because of a mutation: $m_{1\text{ inv}} = \mu b_2 p_{1\text{ inv}}$. In particular, it can be easily found that the ratio of this quantity for the two types reads:

$$\frac{m_{1\text{ inv}}}{m_{2\text{ inv}}} = \frac{c}{r}\frac{p_{1\text{ inv}}}{p_{2\text{ inv}}} \tag{4}$$

Figure 4 inspects the analytical behavior of this expression. Also in this case there is a large range of parameters for which the population evolves to lower values of the invasion fitness.

Evolution in the Chemostat model

As an example for the application of the previous results, we consider a population growing on externally provided resources in a chemostat [34]. We consider a birth-death process where the birth-rate depends on the expected availability of resources, while the death rate is a constant factor. In the deterministic limit the equation reduces to

$$\frac{1}{n_i}\frac{dn_i}{dt} = \frac{\eta_i \alpha_i}{\frac{1}{M}\sum_i n_i \alpha_i} - \delta_i \ . \tag{5}$$

The parameter α_i represents the resource intake rate of allele i, δ_i is a death/dilution rate, while η_i is the efficiency of resource-to-biomass conversion (equivalent to an inverse yield, see Materials and Methods). One can then map this model into our general framework (6).

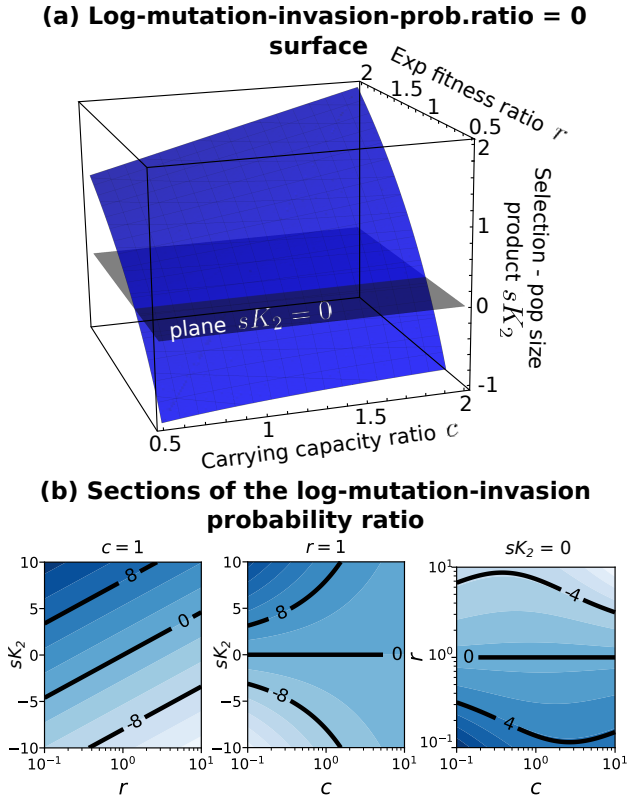

FIG. 4: Behavior of the invasion probability through mutations.

A particularly interesting scenario appears when α is the only parameter which evolves through mutations, while δ or η depend on it. For instance, yield (or, equivalently, efficiency) decreases during selection in experimental evolution [41–43], giving rise to a trade-off between growth rate and yield.

Specifically, we focus on the case $\delta_i/\eta_i = \alpha_i + \alpha_0$. We consider the case where $\alpha_0 \ll 1$ is a small parameter (in principle of the order of $1/M$). This choice implies that the population size at carrying capacity in a clonal population, i.e. $K_i = M\eta_i/\delta_i$, decreases with the intake rate α. This choice reflects the existence of a trade-off between growth rate and yield.

In the deterministic limit, it is easy to see that alleles with higher intake-rate (and therefore with higher invasion fitness) always invade populations with lower values of α. By using using equations (3) and (4), we show that the presence of a large, but finite, allele-dependent total population size can invert this behavior. Moreover, unlike in the evolutionary case, the outcome of the evolutionary process depends on whether the dependency on α is included in the death rate or in the efficiency. We consider here the former case, while we discuss the latter, which nevertheless leads to similar results, in the Supplementary Materials, section 4.

If the intake conversion from the resource to the biomass is constant, η_0, the death rate per-capita can be expressed as $\delta_i = \eta_0(\alpha_i + \alpha_0)$. The computation of the exponential fitness ratio leads to $r = c$. In such a case, there is no difference between the invasion or invasion through mutations. Therefore, both those criteria say that the ratio of the probabilities of fixation is larger than one if

$$\alpha_1 > \alpha_2 \quad \text{or} \quad \alpha_1 < \frac{M\alpha_0}{2\alpha_2}$$

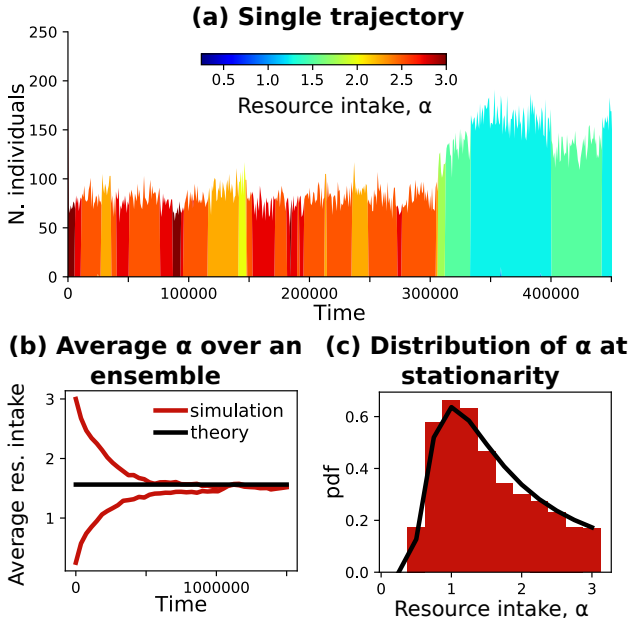

FIG. 5: Evolutionary dynamics of the chemostat with a constant intake rate $\eta_0 = 1$. The resource intake α can mutate to a neighbour $\alpha + \Delta\alpha$ or $\alpha - \Delta\alpha$ with rate $\mu = 2 \cdot 10^{-5}$. It is constrained to be in $[0, 3]$. The other parameters are: $\Delta\alpha = 0.25$, $\alpha_0 = 0.01$, $M = 200$. Panel (a) shows the number of individuals colored by their value of α of a Gillespie simulation. There is no clonal interference since, typically, there is no co-existence of sub-populations with different α. Panel (b) is the average resource intake over 300 realizations of two ensembles starting from different initial conditions. Panel (c) is the distribution of α at stationarity of the 300 realizations.

leading to an evolutionary stable value of the parameter that reads $\alpha^* = \sqrt{\alpha_0 M/2}$.

Figure 5 shows a simulation of this scenario, where α can mutate taking discrete-equispaced values, $\{\alpha_i\}$, with a very small mutation probability that guarantees that periodic selection regime holds.

In this case, one can predict the distribution $p(\alpha)$ at equilibrium assuming a jump process which satisfies the detailed balance: $p(\alpha_i)p(\alpha_i \to \alpha_{i+1}) = p(\alpha_{i+1})p(\alpha_{i+1} \to \alpha_i)$ (details in Supplementary Materials, section 4).

The prediction for the average and for the full distribution are in agreement with the simulation in the panels (b) and (c) of Figure 5. In particular, it is interesting to see in panel (b) that the average intake rate can decrease with time.

Discussion

Here we have studied the evolutionary trajectories of populations in a broad class of models characterizing population self-limitation. It has been introduced a population dynamics framework that encompasses several known models (Logistic, Gompertz, Chemostat and others). In presence of large, but finite, populations sizes, we have shown that the evolutionary trajectory of these population depends only on three quantities (exponential fitness, invasion fitness, and carrying capacities), irrespective of models' specifics.

We obtained this results by assuming a time-scale separation between the total population size and the allele frequencies [24, 27, 29, 31]. This assumption allows to obtain an effective equation that describe the time evolution

of allele frequencies, which depends only on the values of the three evolutionary relevant quantities. This effective description is akin to Kimura's diffusion, to which it reduces if alleles differ only in their invasion fitness or in the limit of strong selection, where variation in exponential fitness and/or carrying capacities becomes effectively irrelevant.

One especially interesting aspect of this effective equation is the role played by the (finite) population size. In Kimura's diffusion limit, population size influences only the strength of drift. While in that context drift masks the effect of selection (e.g., a deleterious mutation has a non-zero fixation probability), it never alters its direction (i.e., a beneficial mutation has always a larger fixation probability than a deleterious one). In our setting, the existence of a finite population size might alter the course of evolution: mutants with lower invasion fitness might be more likely to invade than alleles with an higher invasion fitness.

We explicitly show this effect in the chemostat model in the presence of a metabolic tradeoff. In the deterministic limit, larger resource intakes correspond to higher-fitness and therefore evolution drives to population to higher and higher resource intakes. In presence of a large, yet finite, population size the naive expectation obtained in the deterministic case is not realized. The evolutionary trajectory converge in fact to an optimal value of the intake rate, which we analytically predict. If a clonal population has an initial intake rate larger than the optimal one, evolution will drive the population to decrease the intake rate, and therefore invasion fitness.

Invasion fitness decreases over time because of the presence of a finite population size. This might be reminiscent of the Muller's ratchet [44–46], but it has a radically different origin. In the case of the Muller's ratchet, the decrease in fitness is determined by the fact that mutations only give rise to deleterious mutations, which can get fixed because of the finite population size. The presence of a small fraction of beneficial mutations is enough to balance the effect of deleterious mutations and lead to an overall increase of fitness [47].

In our case, the mechanism in play is radically different. The presence of variation in exponential fitness and/or in the carrying capacity creates an effective force driving the population to higher values of the carrying capacity and lower values of exponential fitness. Lower carrying capacities and higher exponential fitness correspond to higher level of demographic stochasticity (as shown in eq.(2) of the Supplementary Materials). The intuition is that the evolutionary trajectory drives the population toward lower values of demographic stochasticity. This effect is alike to thermophoresis [48] or to what observed in Brownian motion in presence of a position-dependent diffusion: an effective force drive the trajectories to lower values of noise [49]. In our case, the effective force can counter balance the presence of a selection coefficient.

This result highlight the relevance of genetic drift in shaping the evolutionary trajectories. In our case, drift not only affect the speed of evolution [50], but also its direction. One remarkable aspect is that this effect turns out to be model independent and determined only by differences in the exponential fitness and carrying capacity.

The three quantities (invasion fitness, carrying capacity, and exponential fitness) that effectively determine the trajectory of an evolving population are obviously not independent traits. Variation of a given trait can influence one, two or all three of them. For instance, in the example of the chemostat model that we discussed, only one trait, the resource intake, was under selection pressure. But since it influenced all the three quantities the result of evolution was far from trivial.

These results go in the direction of building a model-independent eco-evolutionary theory. The extent at which the specific details of ecological interactions influence the evolutionary outcome is in fact a major limitation to the development a comprehensive general understanding of eco-evolutionary trajectories. Our results present a first

step in this direction, as they describe the evolution of a population limited by a single factor. The next step will be to generalize our framework by considering multiple limiting factors, giving rise to the coexistence of different populations [51]. As a further generalization, one can consider different interaction types, going beyond competition.

To conclude, our work shows that several aspects of the demographic dynamics are details that do not influence the trajectories of an evolving population. Only three life-history, effective, traits matters. Their variation is subject to selection in a non-trivial, drift mediated, way, which might lead to a decrease of what is usually identified as fitness over time.

Material and Methods

Model definition and interpretation of parameters

Let us consider a population with A alleles. The allele abundances n_i, $i = 1, \ldots, A$, can increases/decrease of one unit according to birth/death events whose rates are defined as follows:

$$\begin{aligned} n_i &\to n_i + 1 \ \text{ w. rate } \ n_i \beta\left(z(\mathbf{n})\right) \rho_i \\ n_i &\to n_i - 1 \ \text{ w. rate } \ n_i \beta\left(z(\mathbf{n})\right) \rho_i \frac{\omega\left(z(\mathbf{n})\right)}{\phi_i}. \end{aligned} \tag{6}$$

The two parameters ρ_i and ϕ_i are the *exponential* and *invasion fitness* respectively. The functions $\beta\left(z(\mathbf{n})\right)$, and $\omega\left(z(\mathbf{n})\right)$ are arbitrary, with the constraints of both being positive for $z > 0$, and ω being monotonic increasing. They depend on the abundances $\mathbf{n} = \{n_1, \ldots, n_K\}$ through the following variable:

$$z(\mathbf{n}) = \frac{1}{M} \sum_j n_j \chi_j \ ,$$

where M sets the scale of the population size, and χ_i measures the effect of the abundance of allele i on the growth rate.

The system of competing alleles described by (6) obeys the deterministic dynamics (1), which provides a good description for an infinite population scale M (see Supplementary Materials, section 1). A closer inspection of its behavior is useful to understand the parameter meaning and the long term behavior of the dynamics.

In the regime of a small population, $N = \sum_j n_j \ll M$, the population grows exponentially and there is no interaction between alleles:

$$\frac{1}{n_i} \frac{dn_i}{dt} \approx \rho_i \beta(0) \left(1 - \frac{\omega\left(0\right)}{\phi_i}\right) \ . \tag{7}$$

In the case of $\omega(0) = 0$, which is for instance satisfied by both the Lotka-Volterra and the chemostat dynamics, the allele growth-rate is defined by the *exponential fitness* ρ_i, which therefore describes the growth in absence of population limitation.

As the total population grows, the function $z(\mathbf{n})$ increases. As a consequence, also the function $\omega(z)$ increases, since, by definition, it is monotonically increasing. This ensures a saturation mechanism for the population size. It can be easily shown that the only fixed points are a mass extinction, $n_i = 0 \ \forall i$, and the ones where there is only one surviving allele at carrying capacity $K_j = M\omega^{-1}(\phi_j)/\chi_j$, where ω^{-1} is the inverse function of ω.

Let us consider one of the fixed points with a resident species j and an invader i. The dynamics of the rare mutant i is given by

$$\frac{1}{n_i}\frac{dn_i}{dt} \approx \rho_i \beta\left(\omega^{-1}(\phi_j)\right)\left(1-\frac{\phi_j}{\phi_i}\right) \ .$$

The growth rate of the mutant is positive if and only if $\phi_i > \phi_j$, implying that the surviving allele is the one with the largest *invasion fitness* ϕ.

Effective dynamics

The birth-death model (6) can be approximated, for large M, with an Itô stochastic differential equation for each allele $\dot{n}_i = a_{n_i} + \sqrt{2D_{n_i}} \cdot \xi_i$, where ξ_i is an uncorrelated normal random variable, $\langle \xi_i(t) \rangle = 0$, $\langle \xi_i(t)\xi_j(t') \rangle = \delta_{ij}\delta(t-t')$. The diffusive limit is shown in Supplementary Materials, section 1. The deterministic and diffusion coefficient read:

$$\begin{aligned} a_{n_i} &= n_i \rho_i \beta\left(z\right)\left(1-\frac{\omega\left(z\right)}{\phi_i}\right) \\ D_{n_i} &= \frac{1}{2} n_i \rho_i \beta\left(z\right)\left(1+\frac{\omega\left(z\right)}{\phi_i}\right) \ , \end{aligned} \tag{8}$$

This description becomes particularly useful in the weak selection regime. We can define the invasion fitness as $\phi_i = \phi(1-s_i)$, where $\phi = \phi_1$ represents the fitness of the first species ($s_1 = 0$) and all the other parameters are very close to it. The weak selection regime is realized when $s_i \ll 1$.

We will consider two alleles. We can introduce an effective variable y equal to the first re-scaled abundance: $n_1 = yK_1$, $n_2 = (1-y)K_2$. Imposing the separation of timescales (Supplementary Materials, section 2), one obtains the stochastic differential equation 2, describing the effective stochastic dynamics of the variable y.

Definition of the ecological models

Lotka-Volterra

The competitive Lotka-Volterra model is recovered for $\omega(z) = z$ and $\beta(z) = 1$. The average evolution of the allele abundances reads:

$$\frac{1}{n_i}\frac{dn_i}{dt} = \rho_i\left(1-\frac{\sum_j \chi_j n_j}{M\phi_i}\right) \tag{9}$$

Chemostat

To derive the chemostat dynamics, let us consider an allele i which grows with a birth rate per-capita $b_i = R(\gamma)\alpha_i\eta_i$. This rate depends on a function of the resource concentration $R(\gamma)$, the amount of resource that the allele is able to consume, α_i, and the conversion factor of the resource into biomass η_i. Note that the inverse of this latter quantity corresponds to the yield of the allele. The per-capita death rate is constant, δ_i. We assume that the resource concentration γ quickly reaches a stationary value, where the injection rate is balanced by the consumption of the different species. If the dynamics for the concentration follows $\dot{\gamma} = S - \sum_i \alpha_i R(\gamma) n_i/M$, one can easily get $R(\gamma^*)$ at

the stationary value. It can be substituted in the birth rate for the allele i, and the time and δ_i can be re-scales and by the constant factor S. Equation 5 describes the average dynamics [36].

One can then map this model into our general framework: $\beta(z) = 1/z$, $\omega(z) = z$, $\rho_i = \alpha_i \eta_i$, $\phi_i = \alpha_i \eta_i / \delta_i$, and $\chi_i = \alpha_i$.

Generalized Moran model

The mapping with the Generalized Moran model [31] can be obtained with $\beta(z) = 1$, $\omega(z) = \alpha(1+z)$, $s = 0$ and $\chi_i = 1$. This corresponds to their "quasi-neutrality" case, where α, defined as the ration of death and birth rate is constant for each genotype. The resulting birth-death process is

$$\begin{aligned} n_i &\to n_i + 1 \ \text{ w. rate } \ n_i \rho_i \\ n_i &\to n_i - 1 \ \text{ w. rate } \ n_i \rho_i \alpha \left(1 + \sum_j \frac{n_j}{M} \right), \end{aligned} \tag{10}$$

which are the equations (1) and (2) of the paper [31] at quasi-neutrality and without mutations.

Gompertz growth

A generalization of the Gompertz growth law [38] for competing species is the following:

$$\frac{1}{n_i} \frac{dn_i}{dt} = \alpha_i \log \left(\frac{M k_i}{\sum_j \chi_j n_j} \right), \tag{11}$$

which recovers the classical Gompertz growth dynamics in the case of one allele and $\chi_1 = 1$. The mapping with the general framework can be done as follows: $\beta(z) = 1$, $\omega(z) = \log(z)$, $\rho_i = \alpha_i \log(k_i)$, $\phi_i = \log(k_i)$.

Generalized Lotka-Volterra

The generalized logistic dynamics [39] for competing species can be written as follows:

$$\frac{1}{n_i} \frac{dn_i}{dt} = \rho_i \left(1 - \left(\frac{\sum_j \chi_j n_j}{M k_i} \right)^{\nu} \right), \tag{12}$$

whose mapping reads: $\beta(z) = 1$, $\omega(z) = z^{\nu}$, $\phi_i = k_i^{\nu}$. The simulations of figure 3 are obtained for $\nu = 1/2$.

Von Bertalanffy model

An extension of the Von Bertalanffy model [40] to competing species reads:

$$\frac{1}{n_i} \frac{dn_i}{dt} = p_i \left(\frac{\sum_j \chi_j n_j}{M} \right)^{\alpha - 1} - q_i. \tag{13}$$

It is included in the general framework by choosing $\beta(z) = z^{\alpha-1}$, $\omega(z) = z^{1-\alpha}$, $\rho_i = p_i$, $\phi_i = p_i/q_i$. The simulations of figure 3 are obtained for $\alpha = 2/3$.

---

[1] M. Kimura, Genetics **47**, 713 (1962).

[2] W. J. Ewens, Theoretical population biology **3**, 87 (1972).

[3] J. F. C. Kingman, Stochastic processes and their applications **13**, 235 (1982).

[4] R. R. Hudson, M. Kreitman, and M. Aguadé, Genetics **116**, 153 (1987).

[5] F. Tajima, Genetics **123**, 585 (1989).

[6] S. A. Sawyer and D. L. Hartl, Genetics **132**, 1161 (1992).

[7] Z. Yang and J. P. Bielawski, Trends in ecology & evolution **15**, 496 (2000).

[8] J. H. Gillespie, *Population genetics: a concise guide* (JHU Press, 2004).

[9] W. J. Ewens, *Mathematical population genetics 1: theoretical introduction*, vol. 27 (Springer Science & Business Media, 2012).

[10] S. Wright, Genetics **16**, 97 (1931).

[11] R. A. Fisher, *The genetical theory of natural selection* (nonebbl@id@@russianid@@russian , 1958).

[12] P. A. P. Moran, in *Mathematical proceedings of the cambridge philosophical society* (Cambridge University Press, 1958), vol. 54, pp. 60–71.

[13] S. Karlin and J. McGregor, Proceedings of the National Academy of Sciences of the United States of America **51**, 598 (1964).

[14] C. Cannings, Advances in Applied Probability pp. 260–290 (1974).

[15] J. E. Barrick and R. E. Lenski, Nature Reviews Genetics **14**, 827 (2013).

[16] A. Sanchez and J. Gore, PLoS Biol **11**, e1001547 (2013).

[17] A. R. Rogers and H. Harpending, Molecular biology and evolution **9**, 552 (1992).

[18] O. Hallatschek, P. Hersen, S. Ramanathan, and D. R. Nelson, Proceedings of the National Academy of Sciences **104**, 19926 (2007).

[19] O. J. Burton, B. L. Phillips, and J. M. Travis, Ecology letters **13**, 1210 (2010).

[20] W. J. Ewens, Heredity **22**, 438 (1967).

[21] S. P. Otto and M. C. Whitlock, Genetics **146**, 723 (1997).

[22] L. M. Wahl and P. J. Gerrish, Evolution **55**, 2606 (2001).

[23] Z. Patwa and L. M. Wahl, Journal of The Royal Society Interface **5**, 1279 (2008).

[24] T. L. Parsons and C. Quince, Theoretical population biology **72**, 121 (2007).

[25] T. L. Parsons and C. Quince, Theoretical population biology **72**, 468 (2007).

[26] Y. T. Lin, H. Kim, and C. R. Doering, Journal of Statistical Physics **148**, 647 (2012).

[27] G. W. Constable and A. J. McKane, Physical review letters **114**, 038101 (2015).

[28] T. Chotibut and D. R. Nelson, Physical Review E **92**, 022718 (2015).

[29] T. Chotibut and D. R. Nelson, Journal of Statistical Physics **167**, 777 (2017).

[30] P. Czuppon and A. Traulsen, Journal of mathematical biology **77**, 1233 (2018).

[31] T. L. Parsons, C. Quince, and J. B. Plotkin, Genetics **185**, 1345 (2010).

[32] G. W. Constable, T. Rogers, A. J. McKane, and C. E. Tarnita, Proceedings of the National Academy of Sciences **113**, E4745 (2016).

[33] A. McAvoy, N. Fraiman, C. Hauert, J. Wakeley, and M. A. Nowak, Theoretical population biology **121**, 72 (2018).

[34] H. L. Smith and P. Waltman, *The theory of the chemostat: dynamics of microbial competition*, vol. 13 (Cambridge university press, 1995).

[35] T. L. Parsons and T. Rogers, Journal of Physics A: Mathematical and Theoretical **50**, 415601 (2017).

[36] A. Posfai, T. Taillefumier, and N. S. Wingreen, Physical review letters **118**, 028103 (2017).

[37] B. Gompertz, Philosophical transactions of the Royal Society of London pp. 513–583 (1825).

[38] C. P. Winsor, Proceedings of the National Academy of Sciences of the United States of America **18**, 1 (1932).

[39] F. Richards, Journal of experimental Botany **10**, 290 (1959).

[40] L. Von Bertalanffy, The quarterly review of biology **32**, 217 (1957).

[41] F. Vasi, M. Travisano, and R. E. Lenski, The american naturalist **144**, 432 (1994).

[42] M. Novak, T. Pfeiffer, R. E. Lenski, U. Sauer, and S. Bonhoeffer, The American Naturalist **168**, 242 (2006).

[43] J.-N. Jasmin, M. M. Dillon, and C. Zeyl, Proceedings of the Royal Society B: Biological Sciences **279**, 4382 (2012).

[44] H. J. Muller, Mutation Research/Fundamental and Molecular Mechanisms of Mutagenesis **1**, 2 (1964).

[45] W. Gabriel, M. Lynch, and R. Bürger, Evolution **47**, 1744 (1993).

[46] R. A. Neher and B. I. Shraiman, Genetics **191**, 1283 (2012).

[47] S. Goyal, D. J. Balick, E. R. Jerison, R. A. Neher, B. I. Shraiman, and M. M. Desai, Genetics **191**, 1309 (2012).

[48] R. Piazza, Soft Matter **4**, 1740 (2008).

[49] S. Chapman, Proceedings of the Royal Society of London. Series A, Containing Papers of a Mathematical and Physical Character **119**, 34 (1928).

[50] M. M. Desai and D. S. Fisher, Genetics **176**, 1759 (2007).

[51] B. H. Good, S. Martis, and O. Hallatschek, Proceedings of the National Academy of Sciences **115**, E10407 (2018).